

LEA: Beyond Evolutionary Algorithms via Learned Optimization Strategy

Kai Wu¹ Penghui Liu¹ Jing Liu¹

Abstract

Evolutionary algorithms (EAs) have emerged as a powerful framework for expensive black-box optimization. Obtaining better solutions with less computational cost is essential and challenging for black-box optimization. The most critical obstacle is figuring out how to effectively use the target task information to form an efficient optimization strategy. However, current methods are weak due to the poor representation of the optimization strategy and the inefficient interaction between the optimization strategy and the target task. To overcome the above limitations, we design a learned EA (LEA) to realize the move from hand-designed optimization strategies to learned optimization strategies, including not only hyperparameters but also update rules. Unlike traditional EAs, LEA has high adaptability to the target task and can obtain better solutions with less computational cost. LEA is also able to effectively utilize the low-fidelity information of the target task to form an efficient optimization strategy. The experimental results on one synthetic case, CEC 2013, and two real-world cases show the advantages of learned optimization strategies over human-designed baselines. In addition, LEA is friendly to the acceleration provided by Graphics Processing Units and runs 102 times faster than unaccelerated EA when evolving 32 populations, each containing 6400 individuals.

1. Introduction

Optimization has been an old and essential research topic in history; Many tasks in computer vision, machine learning, and natural language processing can be abstracted as optimization problems. Moreover, many of these problems are black-box, such as neural architecture search (Elsken et al.,

*Equal contribution ¹Xidian University, Xi'an, China. Correspondence to: Penghui Liu <kwu@xidian.edu.cn>.

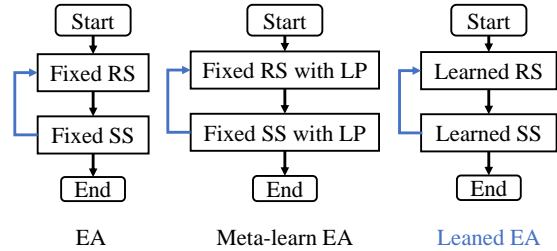


Figure 1. It shows the difference between traditional EA, meta-learn EA, and our proposed LEA. RS represents recombination strategy. SS stands for selection strategy. LP represents learned parameters. LEA learns the update rules and their hyperparameters. Meta-learn EAs only focus on learning the hyperparameters of the fixed update rules. Traditional EAs employ fixed update rules with fixed hyperparameters.

2019) and hyperparameter optimization (Hutter et al., 2019). Various approaches, such as Bayesian optimization (Snoek et al., 2012) and evolutionary algorithms (EAs), including genetic algorithms (Mitchell, 1998; Jin et al., 2019; Khadka & Tumer, 2018; Zhang & Li, 2007; Such et al., 2017; Stanley et al., 2019) and evolution strategies (ES) (Wierstra et al., 2014; Vicol et al., 2021; Hansen & Ostermeier, 2001; Auger & Hansen, 2005; Salimans et al., 2017), have been proposed to deal with these problems in the past.

However, faced with a new black-box optimization task, we need to redesign the EA’s genetic operations to maximize its performance on the target task, resulting in a hand-designed EA with significant application limitations. Most importantly, due to the limitation of expert knowledge, only little target function information is used to assist the design of EA, which makes it challenging to adapt to the target task. Thus, how to automatically design optimization strategies according to new tasks is crucial. Several methods (Shala et al., 2020; Lange et al., 2022) learn some parameters of evolution strategies, not the overall algorithm. However, this strategy only learns part of the update rules and cannot fully represent the whole optimization strategy. Thus, poor representation of the optimization strategy results in the failure to utilize the information of the objective function to form an efficient optimization strategy. Meanwhile, due to the black-box nature of the objective function, the optimization problems designed to guide the construction of optimization

strategies are basically expensive and nonconvex, which is difficult to solve effectively, especially for high-dimensional problems.

Thus, this paper first attempts to develop a learned EA (LEA) to learn to exploit structure in the problem of interest so that LEA can automatically move a random population near the optimal solution for different black-box optimization tasks. LEA solves two key parts: 1) *how to design the efficient model to represent optimization strategies* and 2) *how to effectively train the designed LEA with target task*.

Like EAs, we propose two learned components of LEA to generate and select potential solutions: a convolution-based reasoning module (CRM) and a selection module (SM). CRM ensures the exchange of information between individuals in the population to generate potential solutions. We design a lattice-like environment organizing the population into the modified convolution operators and then employ mirror padding (Goodfellow et al., 2016) to generate the potential offspring. SM updates the population to survive the fittest solutions based on a pairwise comparison between the offspring and the input population regarding their fitness. This process is implemented by employing the mask operator. Then, we design the evolution module (EM) based on CRM and SM to simulate one generation of EAs. Finally, we build the LEA by stacking several EMs to cope with the first issue.

The untrained LEA needs to handle the black-box optimization problem better because it does not contain information about the target function. To overcome the second issue, we design a proper loss function and training dataset. It is difficult to obtain gradient information to assist in the training of LEA. We construct a differentiable and cheap surrogate function set of the target black-box function to avoid querying the expensive function and obtain the information of the target function. The designed loss function maximizes the difference between the initial and output populations to train LEA towards the optimal solution, where the loss function can be optimized by back-propagation.

We test the performance of LEA on nine standard black-box functions, CEC 2013, protein docking problem, and planner mechanic arm problem. Eight EA baselines, Bayesian optimization (Kandasamy et al., 2020), and a learning-to-optimize method for black-box optimization (Cao et al., 2019) are employed as references. The results indicate that LEA can automatically learn efficient optimization strategies on high-fidelity and low-fidelity training datasets. In addition, LEA is transferred to unseen objective functions with different dimensions and populations with different scales during the training stage. The results verify the good generalization capability of LEA. Finally, we demonstrate that LEA is friendly to Graphics Processing Unit (GPU) acceleration; the runtime of LEA on one 1080Ti GPU is

102x faster than standard EA.

2. Related Work

LEA has a strong relationship with EA. Meanwhile, LEA is a new learning-to-optimize (L2O) framework for EA.

EAs. EAs are inspired by the evolution of species and have provided acceptable performance for black-box optimization. There are two essential parts to EAs: 1) crossover and mutation: how to generate individuals with the potential to approach the optimal solution; 2) selection: how to discard individuals with inferior performance while maintaining the ones with superior performance. In the past decades, many algorithmic components have been designed for different tasks in EAs. The performance of algorithms varies towards various tasks, as different optimization strategies may be required given diverse landscapes. Existing methods manually adjust genetic operators’ hyperparameters and design the combination between them (Kerschke et al., 2019; Tian et al., 2020). However, its crossover, mutation, and selection modules can only be designed manually based on expert knowledge and cannot effectively interact with the target task; that is, they cannot change optimization strategies automatically to adapt to new problems through the feedback of the objective function.

L2O for EA. The most related work is about L2O (Chen et al., 2022). This type only learns some hyperparameters of EA, not the overall algorithm. (Shala et al., 2020) meta-learn a policy that configured the mutation step-size parameters of CMA-ES (Hansen & Ostermeier, 2001). LES (Lange et al., 2022) proposed a self-attention-based search strategy to discover effective recombination weights and an MLP to find learning rates for evolution strategies via meta-learning. These schemes are all dealing with low-dimensional black-box problems. In order to train the meta-optimizer, a large number of expensive black-box functions need to be requested, which is very unrealistic. The established black-box objective function for the meta-optimizer is difficult to optimize during training, resulting in a poor representation of the optimization strategy.

3. Learned Evolutionary Algorithm

3.1. Problem Definition

The expensive black-box optimization problem f can be transformed or represented by a minimization problem, and constraints may exist for corresponding solutions:

$$\min f(s|\xi), s.t. x_i \in [d_i, u_i], \forall x_i \in s, \quad (1)$$

where $s = (x_1, x_2, \dots, x_D)$ represents the solution of f while $d = (d_1, d_2, \dots, d_D)$ and $u = (u_1, u_2, \dots, u_D)$ denote the corresponding lower and upper bounds of the solu-

tion’s domain, respectively. ξ is the known parameters of f . We can only use the query-response terminology because the objective function f is a black box without a closed-form formulation in this setting.

Notations. Suppose n individuals of one population ($S = \{s_1, \dots, s_n\}$) be $s_1 = (x_1^1, x_2^1, \dots, x_D^1), \dots, s_n = (x_1^n, x_2^n, \dots, x_D^n)$. G is an abstract function remarking the optimization strategies, and θ is the parameters of G . S_0 is the initial population, and S_t is the output population. LEA determines the optimization strategy θ based on the feature extracted from the optimization task $f(s|\xi)$, which is formulated as $S_t = G_\theta(S_0, f(s|\xi))$. Based on the optimized θ , LEA optimizes $f(s|\xi)$ by G_θ .

3.2. Convolution-based Reasoning Module

We design CRM to ensure that individuals in the population can exchange information to generate the potential solutions near the optimal solution. The corresponding correction to the convolution operator can achieve this goal.

Organize Population into Convolution. We arrange all individuals in a lattice-like environment with a size of $L \times L$. In this case, we represent the population by using a tensor (i, j, d) , where (i, j) locates the position of one individual $S(i, j)$ in the $L \times L$ lattice and d is the dimension information of this individual. Appendix A gives an illustration of the tensor data. The individuals in the lattice are sorted in descending order to construct a population tensor with a consistent pattern (see Figures 7 and 8 of Appendix A). The number of channels in input tensors is $D + 1$, where D is the dimension of the optimization task, and the fitness of individuals occupies one channel. The fitness channel does not participate in the convolution process but is essential for the information selection in the selection module.

How to Design CRM. After organizing the population into a tensor $(L, L, D + 1)$, we modified the depthwise separable convolution (DSC) operator (Chollet, 2017) to generate new individuals by merging information in different dimensions among individuals. The DSC operator includes a depthwise convolution followed by a pointwise convolution. Pointwise convolution maps the output channel of depthwise convolution to a new channel space. When applied to our task, we remove the pointwise convolution in DSC to avoid the information interaction between channels. Eq. (2) provides the details about how to reproduce offspring, and one example is shown in Appendix Figure 9.

$$S'(i, j) = \sum_{k,l} w_{k,l} S(i+k, j+l), \quad (2)$$

where $S'(i, j)$ denotes the individuals in the output population, $S(i, j)$ denotes the individuals in the input population, and $w_{k,l}$ represents the related parameters of convolution

kernels. Moreover, to adapt to optimization tasks with different dimensions, different channels share the same parameters. The parameters within convolution kernels record the strategies learned by this module to reason over available populations given different tasks. There are still two critical issues to address here.

1) *Since there does not exist a consistent pattern in the population, the gradient upon parameters is unstable as well as divergent.* A fitness-sensitive convolution is designed, where the CRM’s attention to available information should be relative to the quality and diversity of the population. $w_{k,l}$ reflects the module’s attention during reasoning and is usually relative to the fitness of individuals. After that, this problem is resolved by simply sorting the population in the lattice based on individuals’ fitness.

2) *Another vital issue is the scale of the offspring.* We conduct padding before the convolution operator to maintain the same scale as the input population. However, filling the tensor of the population with constant values’ 0’ is not proper, as is usually done in computer vision. Instead, mirror padding copies the individuals to maintain the same scale between the offspring and the input population. As the recombination process conducts the information interaction among individuals, copying the individual is better than extending tensors with a constant value. An implementation of mirror padding to the population is given in Figure 10 (see Appendix B).

The size of convolution kernels within CRM determines the number of individuals employed to implement reasoning of $S'(i, j)$. Several essential issues are necessary to be considered, described in Appendix C. After that, this paper employs convolution kernels with commonly used sizes. Different convolution kernels produce corresponding output tensors, while the final offspring are obtained by averaging multiple convolutions’ output. Then, the fitness of this last offspring will be evaluated.

3.3. Selection Module

The selection module updates the population so as to survive the fittest individuals. SM updates individuals based on a pairwise comparison between the offspring and input population regarding their fitness for efficiency and simplicity. S_{i-1} and S'_{i-1} are the input and output populations of CRM, respectively. S_{i-1} and S'_{i-1} contain $D+1$ channels. The first channel stores the fitness value of an individual. Thereafter, a matrix subtraction of fitness channel corresponding to S_{i-1} and S'_{i-1} compares the quality of individuals from S_{i-1} and S'_{i-1} pairwise. A binary mask matrix indicating the selected individual can be obtained based on the indicator function $l_{x>0}(x)$, where $l_{x>0}(x) = 1$ if $x > 0$ and $l_{x>0}(x) = 0$ if $x < 0$. To extract selected individuals

from S_{i-1} and S'_{i-1} , we construct a binary mask tensor by copying and extending the mask matrix to the same shape as S_{i-1} and S'_{i-1} . The selected information forms a new tensor S_i by employing Eq. (3) illustrated in Figure 2.

$$S_t = \text{tile}(l_{x>0}(M_{F'} - M_F)) \bullet S_{t-1} + \text{tile}(1 - l_{x>0}(M_{F'} - M_F)) \bullet S'_{t-1} \quad (3)$$

where the *tile* copy function extends the indication matrix to a tensor with size (L, L, D) , $M_F(M_{F'})$ denotes the fitness matrix of $S_{i-1}(S'_{i-1})$, and \bullet indicates the pairwise multiplication between inputs.

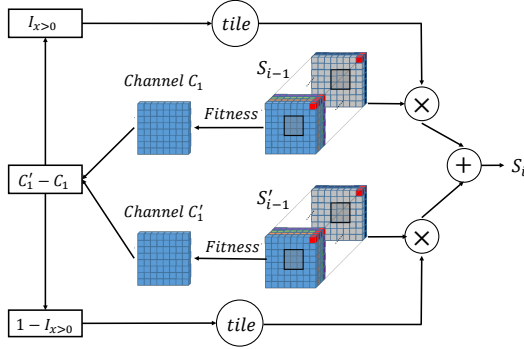


Figure 2. SM. An indication matrix is produced by subtracting the fitness channel (c_1), based on which individuals within the input and output populations can be extracted to form offspring.

3.4. The Structure of LEA

Like EAs, in Figure 3, a learnable module based on CRM and SM is designed to learn optimization strategies, termed evolution module (EM). Then, LEA is established by stacking several EMs to simulate generations within EAs. S_{i-1} is the input population of EM_i . S'_{i-1} is the output of CRM in order to further improve the quality of individuals in the global and local search scopes. Then, SM selects the valuable individuals from S_{i-1} and S'_{i-1} according to their function fitness. Figure 4 provides an intuitive description of data flow in EM.

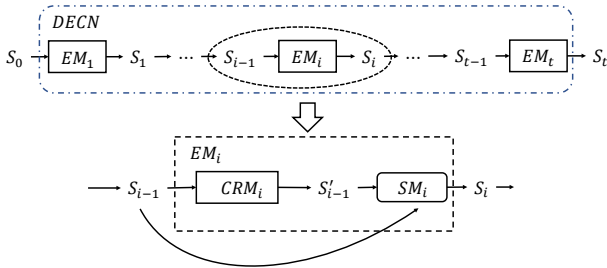


Figure 3. A general view of LEA and EM.

3.5. Training of LEA

LEA with t EMs generates the offspring S_t from the input population S_0 and can be trained based on end-to-end mode. Then, given a proper loss function and training dataset, LEA can be trained to learn optimization strategies towards the objective function $f(s|\xi)$ by the back-propagation. We will generally establish a function set F^{train} to train LEA.

Training Dataset. This paper establishes the training set by constructing a set of differentiable functions related to the optimization objective. This training dataset only contains $(S_0, f_i(s|\xi))$, the initial population and objective function, respectively. f_i represents the i th function in this set. We show the designed training and testing datasets as follows:

$$F^{train} = \{f_1(s|\xi_{1,i}^{train}), \dots, f_m(s|\xi_{m,i}^{train})\}, \quad (4)$$

$$F^{test} = \{F_1(s|\xi_{1,i}^{test}), \dots, F_k(s|\xi_{k,i}^{test})\}$$

where F_1 is not employed in the training stage, and m is the number of functions in F^{train} . $\xi_{m,i}^{train}$ represents the i th different values of ξ in m th function f_m , which is true for any index pair. The initial population S_0 is always randomly generated before optimization. F^{train} is comprised of different functions and has diverse landscapes from F^{test} .

Algorithm 1 Training of LEA

Input: Batch size for Adam, Ω ; Function set for training, F^{train}

Output: Parameters of LEA θ ;

Randomly initialize θ of LEA;

Randomly initialize $\xi_{j,i}^{train}$ to adjust f_j in F^{train} ;

repeat

Randomly initialize a minibatch Ω comprised of K populations S_0 ;

for f_j in F^{train} **do**

Update θ by \mathcal{L}_i given training data (S_0, f_j) ;

end for

Update θ by minimizing $-1/m \sum_j \mathcal{L}_j$;

Re-initialize parameters ξ_j of f_j in F^{train} every T epochs;

until training is finished

Train LEA. LEA attempts to search for individuals with high quality based on the available information. The loss function tells how to adaptively adjust the LEA parameters to generate individuals closer to the optimal solution. According to the Adam (Kingma & Ba, 2014) method, a minibatch Ω is sampled each epoch for the training of LEA upon F^{train} , which is comprised by employing K initialized S_0 for each f_i . We give the corresponding mean loss

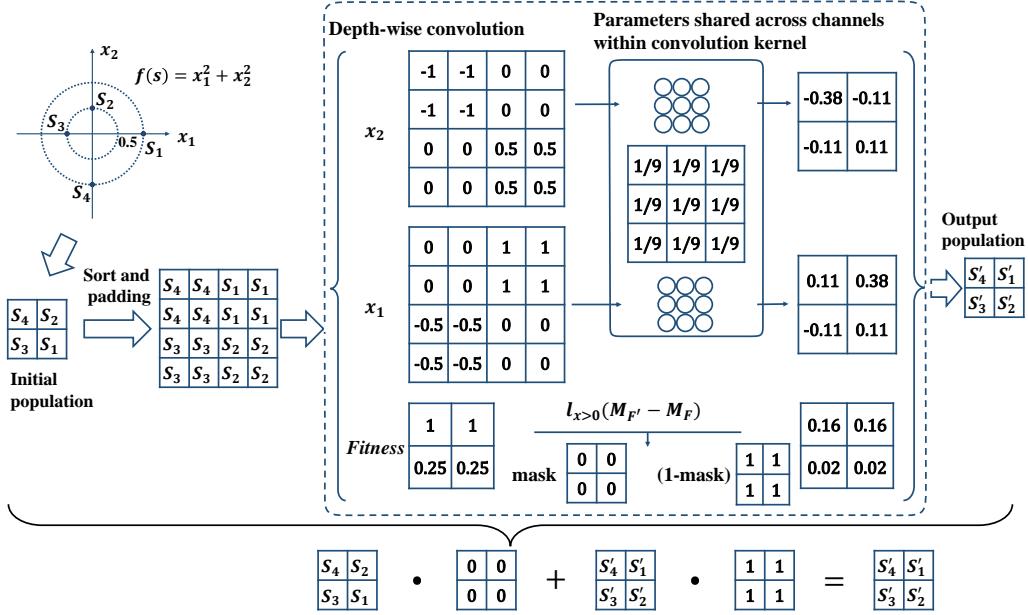


Figure 4. An example to show the data flow in EM. Suppose $f(s = \{x_1, x_2\}, x_i = \{0, 0\}) = (x_1 - 0)^2(x_2 - 0)^2$, $x_i \in [-1, 1]$. L is set to 2. We first transfer the initial population with four individuals to the tensor and then sort and pad it into the new tensor with 16 channels. CRM is employed to generate x_1, x_2 , and the fitness tensor. x_1 and x_2 are handled by parameters shared across channels within a 3×3 convolution kernel. The fitness tensor is handled by Eq. (3). The new tensors of x_1, x_2 , and the fitness tensor are averaged to generate the output.

of minibatch Ω for f_i in F^{train} ,

$$\arg \min_{\theta} - \sum_{S_0 \in \Omega} \frac{\frac{1}{|S_0|} \sum_{s \in S_0} f_i(s|\xi) - \frac{1}{|G_{\theta}(S_0)|} \sum_{s \in G_{\theta}(S_0)} f_i(s|\xi)}{\left| \frac{1}{|S_0|} \sum_{s \in S_0} f_i(s|\xi) \right|} \quad (5)$$

Eq. (5) is to maximize the difference between the initial population and the output population of LEA to ensure that the initial population is close to the optimal solution. Moreover, Eq. (5) are generally differentiable based on the constructed training dataset. Eq. (5) enables LEA to perform the exploitation operation well but does not strongly encourage LEA to explore the fitness landscape. However, we have many options to balance exploration and exploitation. For example, the constructed Bayesian posterior distribution over the global optimum (Cao & Shen, 2020) is added to Eq. (5). Algorithm 1 provides the training process of LEA. After LEA has been trained, LEA can be used to solve the black-box optimization problems since the gradient is unnecessary during the test process.

4. Experiments

4.1. Baselines

Standard EA baselines. Different human-designed genetic algorithms are provided as the reference. EASBX,

EATPC, EAMPC, EASC, and EALC contain the roulette-wheel selection and different crossover operators: simulated binary crossover (SBX), two-point crossover (TPC), multi-point crossover (MPC), shuffle crossover (SC), and linear crossover (LC), respectively. DE (DE/rand/1/bin) (Das & Suganthan, 2010), (μ, λ) -ES and CMA-ES are employed.

Other Black-box Optimization baselines. L2O-swarm (Cao et al., 2019) (a representative L2O method for black-box optimization) and Dragonfly (Kandasamy et al., 2020) (the state-of-the-art Bayesian optimization) are employed.

LEA. Here, we design three models, LEAws3, LEAws30, and LEAnws15. For example, LEAws3 contains 3 EMs, and the parameters of these EMs are consistent (weight sharing). LEAn15 does not share parameters across 15 EMs. The detailed parameters of these models can be found in Table 9 (Appendix D).

Note that we explore whether LEA can obtain better solutions with less function evaluation cost. Therefore, the number of evaluations of all algorithms is set to be small. The setting of the baselines is shown in Appendix E.

4.2. Results on Synthetic Functions

Results on High-fidelity Training Dataset For each function in Appendix Table 8, we produce the training dataset as follows: 1) Randomly initialize the input pop-

Table 1. The compared results on six functions. The value of the objective function is shown in the table, and the optimal solution is bolded. *(*) represents the mean and standard deviation of repeated experiments. The number of function evaluations of LEAws3 is set to 300. The generations of DE, ES, and CMA-ES are set to 100. Thus, the function evaluation cost they use is much higher than that of LEA. Both Dragonfly and L2O-Swarm run to converge.

D	F	LEAws3	DE	ES	CMA-ES	L2O-SWARM	DRAGONFLY
10	F4	1E-6(1E-07)	0.15(0.06)	0.14(0.07)	4E-3(4E-3)	0.30(0.01)	1310(1310)
	F5	1E-3(6E-06)	4.62(1.07)	0.47(0.13)	0.11(0.05)	0.25(8.70E-4)	48.4(9.58)
	F6	8.89(1E2)	244(95.1)	118(235)	1660(2540)	154(243)	9(0)
	F7	0(0)	18.5(3.51)	48.1(8.68)	48.3(7.47)	12.8(5.49)	81.1(24.0)
	F8	0(0)	0.26(0.12)	0.30(0.17)	0.02(0.01)	0.06(3.39E-4)	35.4(22.0)
	F9	1E-3(3E-4)	1.86(0.36)	20.5(0.13)	20.7(0.10)	2.19(0.02)	16.2(3.64)
100	F4	7E-9(4E-11)	8.5E3(396)	9.3E4(8.12E3)	7330(1E3)	0.66(0.04)	1.1E4(3.8E3)
	F5	4E-4(0)	28.2(0.47)	82.5(2.16)	71.8(9.74)	0.96(0.04)	50(0)
	F6	96(0.02)	2.3E8(2.8E7)	2.5E10(3.1E9)	3.4E8(9.5E7)	286(28.5)	99(0)
	F7	0(0)	9.3E3(504)	9.3E4(9.1E3)	8.7E3(1.5E3)	50.6(21.0)	144(13.1)
	F8	0(0)	3.06(0.22)	24.2(2.91)	2.90(0.31)	0.15(1E-3)	125(11.3)
	F9	4E-3(8E-05)	18.9(0.15)	21.4(0.01)	21.4(0.03)	3.06(0.02)	10.5(0.32)

ulation S_0 ; 2) Randomly produce a shifted objective function $f_i(s|\xi)$ by adjusting the corresponding location of optima—namely, adjusting the parameter ξ ; 3) Evaluate S_0 by $f_i(s|\xi)$; 4) Repeat Steps 1)-3) to generate the corresponding dataset. For example, we show the designed training and testing datasets for the F4 function as follows:

$$\begin{aligned} F^{train} &= \{F4(s|\xi_1^{train}), \dots, F4(s|\xi_m^{train})\}, \\ F^{test} &= \{F4(s|\xi^{test})\} \end{aligned} \quad (6)$$

F^{train} and F^{test} are comprised of the same essential function but vary in the location of optima obtained by setting different combinations of ξ (called b_i in Table 8). F^{train} is considered as the high-fidelity surrogate functions of F^{test} .

Here, $D = \{10, 100\}$ and $L = 10$. The results of LEAws3 and compared methods are provided in Table 1. LEA outperforms compared methods by a large margin. This is because we use a high-fidelity surrogate function of the target black-box function to train LEA. The trained LEA contains an optimization strategy that is more tailored to the task. We take a two-dimensional F4 function as an example to verify that LEA can indeed advance the optimization (see Figure 11 in Appendix F). As the iteration proceeds, LEA converges fast and enables better performance with fewer function evaluations.

We also discuss the results to show the effectiveness of LEAws30 compared with traditional GAs. The results for F9 are provided in Figure 5. The results for functions F4-F8 are shown in Figure 12 (Appendix G). As can be seen, the convergence curve of LEAws30 is below the curves of EASBX, EATPC, EAMPC, EASC, and EALC. The performance of LEAws30 surpasses these human-designed GAs.

Results on Low-fidelity Training Dataset Accurate high-fidelity surrogate functions are difficult to obtain.

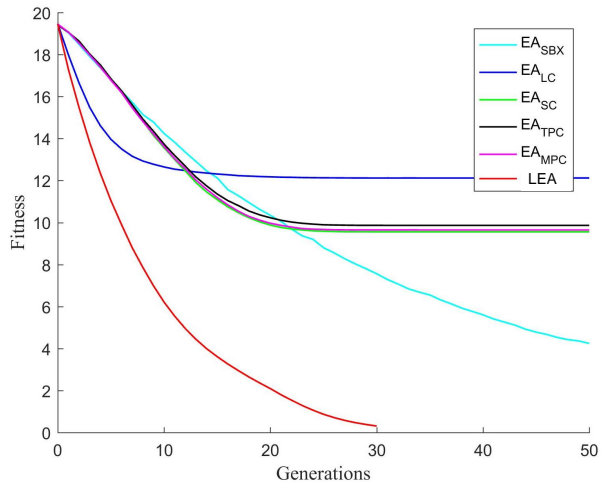


Figure 5. Experimental results are obtained upon F9 in Table 8 when $D = 10$. The generation of algorithms is set to 50, and LEA only evolves for 30 generations. This figure’s experimental results are obtained by averaging over 640 independent runs (batch size = 32).

Therefore, we train LEA on low-fidelity surrogate functions shown in Table 7 and test it on each function in Table 8. The results are shown in Table 2. For example, we show the designed training and testing datasets for the F4 function as follows:

$$\begin{aligned} F^{train} &= \{F1(s|\xi_{1,i}), F2(s|\xi_{2,i}), F3(s|\xi_{3,i})\}, \\ F^{test} &= \{F4(s|\xi^{test})\} \end{aligned} \quad (7)$$

Meanwhile, we also test the impact of different architectures on LEA, including the different number of layers and whether weights are shared between layers.

LEAws30 outperforms LEAws3 in all cases, demonstrating

Table 2. The performance of different LEA.

D	F	LEAws3	LEAws30	LEAN15
10	F4	53.8(14.3)	1.17(0.58)	0.09(0.02)
	F5	4.26(0.61)	0.59(0.16)	0.19(0.03)
	F6	4.5(2.3E4)	131(67.1)	17.0(2.88)
	F7	24.4(4.01)	0.35(0.22)	5.93(1.40)
	F8	1.48(0.14)	0.29(0.08)	0.17(0.04)
	F9	4.33(0.41)	0.91(0.32)	0.22(0.04)
100	F4	1.15E4(744)	2.19E3(148)	67.4(9.09)
	F5	25.0(0.92)	10.4(0.39)	2.22(0.15)
	F6	3E8(4E7)	1E7(2E6)	2E4(5E3)
	F7	776(19.2)	549(18.3)	81.5(11.9)
	F8	105(6.12)	20.9(1.17)	1.58(0.08)
	F9	11.6(0.21)	6.79(0.14)	3.77(0.16)

that deep architectures have stronger representation capabilities and can build a more accurate optimization strategy. LEAN15 outperforms LEAws3 and LEAws30 when $D = 100$. This case is more complex than the case with $D = 10$. Although the number of layers of LEAN15 is lower than that of LEAws30, its representation ability is stronger than that of LEAws30 because it does not share weights. However, when the number of layers becomes larger, this architecture is more difficult to train. The performance of LEA is proportional to the fitness landscape similarity between the training set and the problem. When new problem attributes are not available in the training set, LEA can still perform better. However, if extreme attributes are not available, then LEA can be the less satisfactory performance for functions with this attribute. These results show that the optimization strategy learned by LEA has good generality and is transferable to many unseen objective functions.

Generalization Ability of LEA We validate the generalization ability of the trained LEAws3 model to many different optimization scenarios (such as different tasks, populations with different dimensions (D), and different scales (L)). The parameters of EALC are adjusted well at $D = 2$ and $L = 10$, and then generalized to other situations. F^{train} with $D = 2$ and $L = 10$ is generated based on functions in Table 7, and F^{test} is generated based on functions in Table 8. The detailed results of Table 3 are shown in Appendix 10. LEAws3 outperforms EALC, which indicates the optimization strategy learned by LEA has a good generalization ability to other unseen objective functions and different optimization scenarios: populations with different dimensions and different scales. In this case, LEA has accumulated some general optimization experience. It is worth noting that this tested LEAws3 is trained under a 2-dimensional optimization environment. However, its performance on high-dimensional problems has declined, but it performs well.

Table 3. The compared results of LEAws3 and EALC. w/t/l represents win/tie/loss. The results are obtained through averaging over 640 (batch size=32) independent results.

D	FUNCTION	L			
		10	20	40	80
2	F4-F9	6/0/0	6/0/0	6/0/0	6/0/0
10	F4-F9	6/0/0	6/0/0	6/0/0	6/0/0
30	F4-F9	6/0/0	6/0/0	6/0/0	6/0/0
50	F4-F9	6/0/0	6/0/0	6/0/0	6/0/0
100	F4-F9	6/0/0	6/0/0	6/0/0	6/0/0
500	F4-F9	6/0/0	6/0/0	6/0/0	6/0/0

Table 4. The compared results in CEC2013.

ALGORITHM (W/T/L)	CECF1-CECF28
EATPC vs LEANWS15	3/2/23
EAMPC vs LEANWS15	3/3/22
EASC vs LEANWS15	3/3/22
EALC vs LEANWS15	1/6/21
EASBX vs LEANWS15	2/3/23

Results on CEC2013 We further investigate the generalization ability of LEA on more complex tasks unseen during the training stage. We provide the experimental results obtained upon CEC2013 with 28 functions (Liang et al., 2013) in Table 4. The detailed results are shown in 11 (see Appendix H). LEANws15 performs no worse than human-designed genetic operators and provides the best results in 24 out of 28 cases. These results show that the optimization strategy learned by LEA has good generality and is transferable to many unseen objective functions.

Accelerating LEA with GPU To display the adaptability of LEA to GPUs, we offer the average runtime (second) of LEA and unaccelerated EA for three generations in Appendix Table 12 (See Appendix I for more results). LEA is around 102 times faster than EA.

Table 5. The compared results on protein docking problem.

METHODS	1ATN_7	2JEL_1	7CEL_1
CMA-ES	-6240(100)	-6260(51.8)	-6170(18.4)
ES	-6200(48.1)	-6210(5.05)	-6180(2.47)
DE	-6260(58.1)	-6220(29.2)	-6140(20.5)
DRAGONFLY	-6160(4.3)	-6120(2.9)	-6103(2.0)
LEAWS3	-6261(96.71)	-6250(84.38)	-6193(84.66)

4.3. Results on Protein Docking

We consider the *ab initio* protein docking problem (Smith & Sternberg, 2002), which is formulated as optimizing the Gibbs binding free energy for conformation s : $f(s) = \nabla G(s)$. We calculate the energy function in a CHARMM

Table 6. The results of planar mechanical arm. *gen* is the number of generations for EAs.

CASE	<i>gen</i>	<i>r</i>	DE	ES	CMA-ES	L2O-SWARM	LEAws3
SC	10	100	2.96(1.63)	11.2(4.70)	236(46.8)	40.4(3.89)	0.42(0.22)
		300	11.3(14.7)	45.3(43.3)	243(125)	69.5(3.77)	1.04(1.25)
	50	100	1.28(0.60)	10.7(5.91)	2.42(0.65)	40.4(3.89)	0.42(0.22)
		300	1.54(0.89)	42.0(41.0)	4.06(6.54)	69.5(3.77)	1.04(1.25)
	100	100	1.20(0.64)	10.6(5.58)	1.36(0.35)	40.4(3.89)	0.42(0.22)
		300	1.38(0.71)	44.9(43.3)	1.38(0.41)	69.5(3.77)	1.04(1.25)
CC	100	100	0.81(0.47)	8.95(6.42)	0.76(0.20)	31.9(1.78)	0.38(0.25)
		300	6.15(12.2)	47.8(56.0)	0.87(0.37)	89.1(1.96)	8.27(21.3)

19 force field as in (Moal & Bates, 2010). We parameterize the search space as $s \in R^{12}$ as in (Cao & Shen, 2020). The training set includes 125 instances (see Appendix J for detailed information). The testing set contains 1ATN_7, 2JEL_1, and 2JEL_1 of different levels of docking difficulty. For example, we show the designed training and testing datasets for 1ATN_7 as follows:

$$F^{train} = \{f(s|\xi_1), \dots, f(s|\xi_{125})\}, F^{test} = \{f(s|\xi^{test})\} \quad (8)$$

where ξ represents different instances of protein-protein complexes.

The experimental results reported in Table 5 demonstrate that LEA outperforms L2O-swarm, Dragonfly, DE, CMA-ES, and ES in all three cases. Since L2O-swarm has no elite retention mechanism, its result is worse than the optimal value of the initial population.

4.4. Results on Planar Mechanical Arm

The planner mechanic arm problem (Cully et al., 2015; Mouret & Maguire, 2020) is to find the suitable sets of angles ($\alpha \in R^D$) and lengths ($\beta \in R^D$) such that the distance $f(L, \alpha, p)$ from the top of the mechanic arm to the target position p is the smallest. Here, $D = 100$. We design two groups of experiments.

1) *Simple Case (SC)*. We fixed the length of each mechanic arm as ten and only searched for the optimal α . We randomly selected 600 target points within the range of $r \leq 1000$, where r represents the distance from the target point to the origin of the mechanic arm, as shown in Figure 13 (see Appendix K). In the testing process, we extracted 128 target points in the range of $r \leq 100$ and $r \leq 300$, respectively, for testing. We show the designed training and testing datasets as follows:

$$F^{train} = \{f(\alpha|p_1), \dots, f(\alpha|p_{600})\}, \quad (9)$$

$$F^{test} = \{f(\alpha|p_1^{test}), \dots, f(\alpha|p_{128}^{test})\}$$

2) *Complex Case (CC)*. We search for β and α at the same time. We show the training and testing datasets as follows:

$$F^{train} = \{f((\beta, \alpha)|p_1), \dots, f((\beta, \alpha)|p_{600})\}, \quad (10)$$

$$F^{test} = \{f((\beta, \alpha)|p_1^{test}), \dots, f((\beta, \alpha)|p_{128}^{test})\}$$

We evaluate the performance of the algorithm by $\sum_{f \in F^{test}} f/128$. The experimental results are shown in Table 6. Note that Dragonfly performs poorly due to the high dimension of this problem. In simple cases, LEAws3 outperforms all baselines. Nevertheless, for complex cases, LEAws3 outperforms all baselines when $r \leq 100$. However, when $r \leq 300$, LEAws3 outperforms ES and L2O-Swarm and is weaker than DE and CMA-ES. As shown in Table 2, the performance of LEAws3 is worse than LEA15. When we use LEA15 to optimize the complex case, its result is 0.54(0.26), which is better than all baselines.

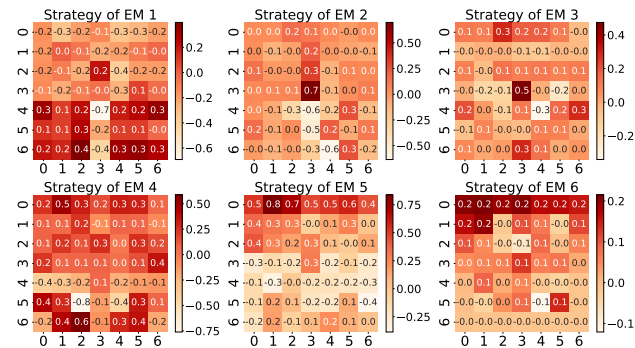


Figure 6. Visualization of the 7×7 convolution kernel.

4.5. Visualization of LEA

We visualize and analyze the optimization strategies learned by LEAws6. LEAws6 is trained on Appendix Table 7. The learnable parameters of LEA are the convolution kernel of the CRM module. Therefore, we choose a 7×7 convolution kernel for display. The convolution kernel represents the solution generation strategy learned by LEA. From EM1 to EM6, the focus area of the optimization strategy is constantly changing. EM1 focuses on the poor and promising areas in terms of function fitness, moves to the middle area (EM2), and then gradually moves to the area with the better function values. Therefore, LEA first focuses on "exploration" and then gradually shifts to "exploitation". The transformation of the focus of the optimization strategy reflects the dynamic balance between "exploration" and "exploitation" of LEA and proves the intelligence of LEA, which is an advantage that traditional EA does not have.

5. Conclusions

We successfully designed LEA to learn optimization strategies for black-box optimization automatically. The better performance than traditional EAs and L2O-based methods demonstrates that LEA achieves better performance with less computational cost. Moreover, LEA has a strong generalization ability to unseen tasks with different scales and dimensions. The limitations are discussed in Appendix L.

References

- Auger, A. and Hansen, N. A restart cma evolution strategy with increasing population size. In *2005 IEEE Congress on Evolutionary Computation*, volume 2, pp. 1769–1776, 2005.
- Blank, J. and Deb, K. pymoo: Multi-objective optimization in python. *IEEE Access*, 8:89497–89509, 2020.
- Cao, Y. and Shen, Y. Bayesian active learning for optimization and uncertainty quantification in protein docking. *Journal of chemical theory and computation*, 16(8):5334–5347, 2020.
- Cao, Y., Chen, T., Wang, Z., and Shen, Y. Learning to optimize in swarms. *Advances in Neural Information Processing Systems*, 32:15044–15054, 2019.
- Chen, T., Chen, X., Chen, W., Heaton, H., Liu, J., Wang, Z., and Yin, W. Learning to optimize: A primer and a benchmark. *Journal of Machine Learning Research*, 23: 1–59, 2022.
- Cheng, J. R. and Gen, M. Accelerating genetic algorithms with gpu computing: A selective overview. *Computers & Industrial Engineering*, 128:514–525, 2019.
- Chollet, F. Xception: Deep learning with depthwise separable convolutions. In *Proceedings of the IEEE conference on computer vision and pattern recognition*, pp. 1251–1258, 2017.
- Cully, A., Clune, J., Tarapore, D., and Mouret, J.-B. Robots that can adapt like animals. *Nature*, 521:503–507, 2015.
- Das, S. and Suganthan, P. N. Differential evolution: A survey of the state-of-the-art. *IEEE transactions on Evolutionary Computation*, 15(1):4–31, 2010.
- Elsken, T., Metzen, J. H., and Hutter, F. Neural architecture search: A survey. *The Journal of Machine Learning Research*, 20(1):1997–2017, 2019.
- et.al., J. geatpy: The genetic and evolutionary algorithm toolbox with high performance in python, 2020.
- Goodfellow, I., Bengio, Y., and Courville, A. *Deep Learning*. MIT press, 2016.
- Hansen, N. and Ostermeier, A. Completely derandomized self-adaptation in evolution strategies. *Evolutionary Computation*, 9(2):159–195, 2001.
- Huang, Y., Feng, L., Qin, A. K., Chen, M., and Tan, K. C. Towards large-scale evolutionary multi-tasking: A gpu-based paradigm. *IEEE Transactions on Evolutionary Computation*, pp. 1–1, 2021. doi: 10.1109/TEVC.2021.3110506.
- Hutter, F., Kotthoff, L., and Vanschoren, J. *Automated machine learning: methods, systems, challenges*. Springer Nature, 2019.
- Hwang, H., Vreven, T., Janin, J., and Weng, Z. Protein-protein docking benchmark version 4.0. *Proteins: Structure, Function, and Bioinformatics*, 78(15):3111–3114, 2010.
- Jin, C. and Qin, A. K. A gpu-based implementation of brain storm optimization. In *2017 IEEE Congress on Evolutionary Computation (CEC)*, pp. 2698–2705. IEEE, 2017.
- Jin, Y., Wang, H., Chugh, T., Guo, D., and Miettinen, K. Data-driven evolutionary optimization: An overview and case studies. *IEEE Transactions on Evolutionary Computation*, 23(3):442–458, 2019. doi: 10.1109/TEVC.2018.2869001.
- Kandasamy, K., Vysyaraju, K. R., Neiswanger, W., Paria, B., Collins, C. R., Schneider, J., Poczos, B., and Xing, E. P. Tuning hyperparameters without grad students: Scalable and robust bayesian optimisation with dragonfly. *Journal of Machine Learning Research*, 21(81):1–27, 2020.
- Kerschke, P., Hoos, H. H., Neumann, F., and Trautmann, H. Automated algorithm selection: Survey and perspectives. *Evolutionary Computation*, 27(1):3–45, 2019. doi: 10.1162/evco.a.00242.
- Khadka, S. and Tumer, K. Evolution-guided policy gradient in reinforcement learning. In Bengio, S., Wallach, H., Larochelle, H., Grauman, K., Cesa-Bianchi, N., and Garnett, R. (eds.), *Advances in Neural Information Processing Systems*, volume 31. Curran Associates, Inc., 2018.
- Kingma, D. P. and Ba, J. Adam: A method for stochastic optimization. *arXiv preprint arXiv:1412.6980*, 2014.
- Lange, R. T., Schaul, T., Chen, Y., Zahavy, T., Dallibard, V., Lu, C., Singh, S., and Flennerhag, S. Discovering evolution strategies via meta-black-box optimization. *arXiv preprint arXiv:2211.11260*, 2022.
- Liang, J. J., Qu, B. Y., Suganthan, P. N., and Hernández-Díaz, A. G. Problem definitions and evaluation criteria for the cec 2013 special session on real-parameter optimization. *Computational Intelligence Laboratory, Zhengzhou University, Zhengzhou, China and Nanyang Technological University, Singapore, Technical Report*, 201212(34): 281–295, 2013.
- Mitchell, M. *An introduction to genetic algorithms*. MIT press, 1998.
- Moal, I. H. and Bates, P. A. Swarmdock and the use of normal modes in protein-protein docking. *International Journal of Molecular Sciences*, 11(10):3623–3648, 2010.

- Mouret, J.-B. and Maguire, G. Quality diversity for multi-task optimization. *Proceedings of the 2020 Genetic and Evolutionary Computation Conference*, 2020.
- Pierce, B. G., Wiehe, K., Hwang, H., Kim, B.-H., Vreven, T., and Weng, Z. Zdock server: interactive docking prediction of protein–protein complexes and symmetric multimers. *Bioinformatics*, 30(12):1771–1773, 2014.
- Qin, K., Raimondo, F., Forbes, F., and Ong, Y. S. An improved cuda-based implementation of differential evolution on gpu. In *Proceedings of the 14th Annual Conference on Genetic and Evolutionary Computation*, pp. 991–998, 2012.
- Salimans, T., Ho, J., Chen, X., Sidor, S., and Sutskever, I. Evolution strategies as a scalable alternative to reinforcement learning. *arXiv preprint arXiv:1703.03864*, 2017.
- Shala, G., Biedenkapp, A., Awad, N., Adriaensen, S., Lindauer, M., and Hutter, F. Learning step-size adaptation in cma-es. In *International Conference on Parallel Problem Solving from Nature*, pp. 691–706. Springer, 2020.
- Smith, G. R. and Sternberg, M. J. Prediction of protein–protein interactions by docking methods. *Current opinion in structural biology*, 12(1):28–35, 2002.
- Snoek, J., Larochelle, H., and Adams, R. P. Practical bayesian optimization of machine learning algorithms. In Pereira, F., Burges, C., Bottou, L., and Weinberger, K. (eds.), *Advances in Neural Information Processing Systems*, volume 25. Curran Associates, Inc., 2012.
- Stanley, K. O., Clune, J., Lehman, J., and Miikkulainen, R. Designing neural networks through neuroevolution. *Nature Machine Intelligence*, 1(1):24–35, 2019.
- Such, F. P., Madhavan, V., Conti, E., Lehman, J., Stanley, K. O., and Clune, J. Deep neuroevolution: Genetic algorithms are a competitive alternative for training deep neural networks for reinforcement learning. *arXiv preprint arXiv:1712.06567*, 2017.
- Tian, Y., Peng, S., Zhang, X., Rodemann, T., Tan, K. C., and Jin, Y. A recommender system for metaheuristic algorithms for continuous optimization based on deep recurrent neural networks. *IEEE Transactions on Artificial Intelligence*, 1(1):5–18, 2020. doi: 10.1109/TAI.2020.3022339.
- Vassiliades, V. and Mouret, J.-B. Discovering the elite hypervolume by leveraging interspecies correlation. *Proceedings of the Genetic and Evolutionary Computation Conference*, 2018.
- Vassiliades, V., Chatzilygeroudis, K., and Mouret, J.-B. Using centroidal voronoi tessellations to scale up the multi-dimensional archive of phenotypic elites algorithm. *IEEE Transactions on Evolutionary Computation*, 22:623–630, 2018.
- Vicol, P., Metz, L., and Sohl-Dickstein, J. Unbiased gradient estimation in unrolled computation graphs with persistent evolution strategies. In *International Conference on Machine Learning*, pp. 10553–10563. PMLR, 2021.
- Wierstra, D., Schaul, T., Glasmachers, T., Sun, Y., Peters, J., and Schmidhuber, J. Natural evolution strategies. *Journal of Machine Learning Research*, 15(1):949–980, 2014.
- Zhang, Q. and Li, H. Moea/d: A multiobjective evolutionary algorithm based on decomposition. *IEEE Transactions on Evolutionary Computation*, 11(6):712–731, 2007.

A. How to Organize a population into a tensor

As shown in Figure 7, individuals in the lattice are sorted in descending order to construct a population tensor with a consistent pattern. Suppose a population $S = s_1, s_2, \dots, s_{L \times L}$ and $f(s_1) < f(s_2) < \dots < f(s_{L \times L})$, where $f(s)$ is a minimization task. $s_1, s_2, \dots, s_{L \times L}$ are arranged in descending order within the $L \times L$ lattice.

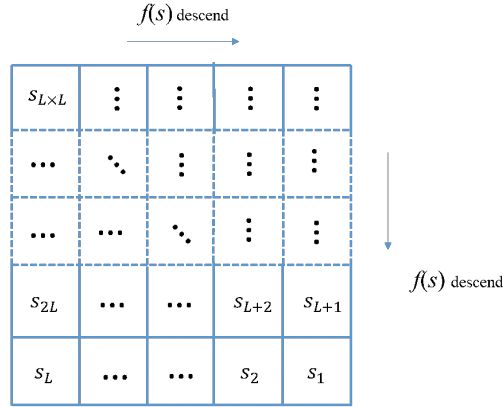


Figure 7. Organizing a population into a tensor.

Figure 8 gives an illustration of the tensor data. As can be seen, the number of channels of input tensors is $D+1$, where D is the dimension of the optimization task, and the fitness of individuals occupies one channel. The fitness channel does not participate in the convolution process but is essential for the selection module in LEA for the information selection.

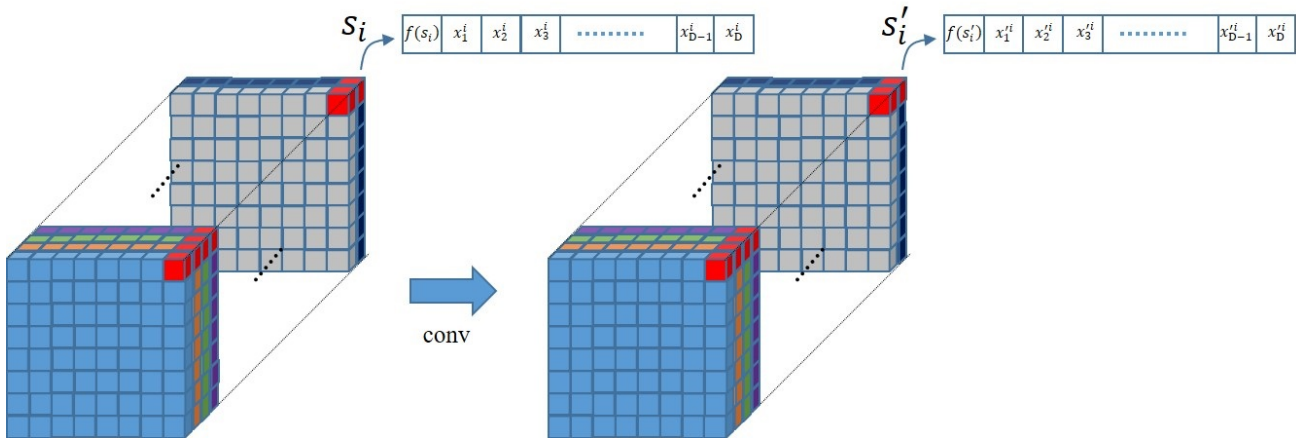


Figure 8. The realization of similar functions as recombination operators based on convolution operator. Convolution kernels slip over the whole $L \times L$ lattice and conduct the information interaction within the neighborhood of (i, j) . For the picture on the left, the small red square with many channels represents S_i .

B. Population Arrangement

Figure 9 gives an example of population arrangement and padding for the problem $\min f(s) = x_1 \times x_1$, where $s = x_1, x_1 \in [0, 10]$. The blue part marks the population arranged in a 10×10 lattice, while the gray region marks the mirror padding part.

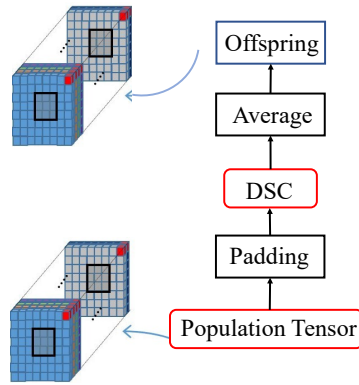


Figure 9. Reproduction of the offspring based on CRM.

C. Several Essential Issues about CRM

There are several essential issues necessary to be considered.

10.	10.	9.9	9.8	9.7	9.6	9.5	9.4	9.3	9.2	9.1	9.1
10.	10.	9.9	9.8	9.7	9.6	9.5	9.4	9.3	9.2	9.1	9.1
9.0	9.0	8.9	8.8	8.7	8.6	8.5	8.4	8.3	8.2	8.1	8.1
8.0	8.0	7.9	7.8	7.7	7.6	7.5	7.4	7.3	7.2	7.1	7.1
7.0	7.0	6.9	6.8	6.7	6.6	6.5	6.4	6.3	6.2	6.1	6.1
6.0	6.0	5.9	5.8	5.7	5.6	5.5	5.4	5.3	5.2	5.1	5.1
5.0	5.0	4.9	4.8	4.7	4.6	4.5	4.4	4.3	4.2	4.1	4.1
4.0	4.0	3.9	3.8	3.7	3.6	3.5	3.4	3.3	3.2	3.1	3.1
3.0	3.0	2.9	2.8	2.7	2.6	2.5	2.4	2.3	2.2	2.1	2.1
2.0	2.0	1.9	1.8	1.7	1.6	1.5	1.4	1.3	1.2	1.1	1.1
1.0	1.0	0.9	0.8	0.7	0.6	0.5	0.4	0.3	0.2	0.1	0.1
1.0	1.0	0.9	0.8	0.7	0.6	0.5	0.4	0.3	0.2	0.1	0.1

Figure 10. Population arrangement and padding.

1) **How many individuals should participate in the CRM reasoning progress.** It remains a challenge to implement information reasoning over multi-individuals in EAs. In most recombination operators, the participant number is usually set to 2. However, based on the gradient information provided by the back-propagation, it is easy to control an individual’s element by adjusting $w_{k,l}$.

2) **How to integrate the offspring produced by different convolution kernels.** Since the convolution operation can be transformed as a multiplication between matrices, simply averaging over the results output by different convolution kernels does not influence the training process. For example, $a_1Co^1x_1^i + a_2Co^2x_2^i + a_3Co^3x_3^i \leftrightarrow Co^1x_1^i + Co^2x_2^i + Co^3x_3^i$, where x_1^i, x_2^i , and x_3^i are input elements of s_i , a_1, a_2 , and a_3 are the constant, and Co denotes the convolution matrix.

3) **How many convolution kernels should be used within CRM.** We suppose that these are three convolution kernels for x . We can find that the outcome $a_1Co_{3 \times 3}^1x + a_2Co_{3 \times 3}^2x + a_3Co_{3 \times 3}^3x$ is equivalent to $a'Co_{3 \times 3}x$. The output of multiple convolution kernels can be replaced by one convolution kernel. Thus, the number of convolution kernels of the same size

has no apparent influence on LEA.

4) **The impact of neighborhood recombination operation.** The neighborhood recombination operation has been commonly accepted in EAs to alleviate the selection pressure and prevent the premature convergence of populations. Moreover, the receptive field of convolution kernels expands as the number of layers increases. Thus, LEA can learn efficient optimization strategies across generations.

D. Nine Synthetic Functions and Parameters

Table 7. Training functions.

ID	FUNCTIONS	RANGE
F1	$\sum_i w_i \sin(x_i - b_i) $	$x \in [-10, 10], b \in [-10, 10]$
F2	$\sum_i x_i - b_i $	$x \in [-10, 10], b \in [-10, 10]$
F3	$\sum_i (x_i - b_i) - (x_{i+1} - b_{i+1}) + \sum_i x_i - b_i $	$x \in [-10, 10], b \in [-10, 10]$

Table 8. Testing Functions. F4(Sphere); F5(Mix); F6(Rosenbrock); F7(Rastrigin); F8(Griewank); 9(Ackley).

ID	FUNCTIONS	RANGE
F4	$\sum_i z_i^2, z_i = x_i - b_i$	$x \in [-100, 100], b \in [-50, 50]$
F5	$\max\{ z_i , 1 \leq i \leq D\}, z_i = x_i - b_i$	$x \in [-100, 100], b \in [-50, 50]$
F6	$\sum_{i=1}^{D-1} (100(z_i^2 - z_{i+1})^2 + (z_i - 1)^2), z_i = x_i - b_i$	$x \in [-100, 100], b \in [-50, 50]$
F7	$\sum_{i=1}^D (z_i^2 - 10 \cos(2\pi z_i) + 10), z_i = x_i - b_i$	$x \in [-5, 5], b \in [-2.5, 2.5]$
F8	$\sum_{i=1}^D \frac{z_i^2}{4000} - \prod_{i=1}^D \cos(\frac{z_i}{\sqrt{i}}) + 1, z_i = x_i - b_i$	$x \in [-600, 600], b \in [-300, 300]$
F9	$-20 \exp(-0.2 \sqrt{\frac{1}{D} \sum_{i=1}^D z_i^2}) - \exp(\frac{1}{D} \sum_{i=1}^D \cos(2\pi z_i)) + 20 + \exp(1), z_i = x_i - b_i$	$x \in [-32, 32], b \in [-16, 16]$

Table 9. Experimental setup for LEAws30, LEAws3, and LEAnws15. In LEAws3, parameters of these three convolution kernels are consistent across different EMs (weight sharing). Moreover, during the training process, the 2-norm of gradients is clipped to be not larger than 10, and the learning rate ($lr = 0.01$) shrinks every 100 epochs. The shrinking rate is set to 0.9. The generation of these reference algorithms is set to 100, while LEAws3 only evolves the population with 3 EMs. 5000 epochs are conducted during the training process. All experimental studies are performed on a Linux PC with Intel Core i7-10700K CPU at 3.80GHz and 32GB RAM.

MODEL	L	D	K	EMS	CONVOLUTION KERNELS	lr	EPOCHS	T	WEIGHT SHARE	GRADIENT NORM
LEAws30	10	10	32	30	$3 \times 3: u = 0, \sigma = 0.5$	0.01	10000	10	TRUE	10
					$5 \times 5: u = 0, \sigma = 0.5$					
					$7 \times 7: u = 0, \sigma = 0.5$					
LEAws3	10	2	32	3	$3 \times 3: u = 0, \sigma = 0.5$	0.0005	5000	10	TRUE	10
					$5 \times 5: u = 0, \sigma = 0.5$					
					$7 \times 7: u = 0, \sigma = 0.5$					
LEAnws15	10	30	16	15	$3 \times 3: u = 0, \sigma = 0.5$	0.0005	2000	10	FALSE	10
					$5 \times 5: u = 0, \sigma = 0.5$					
					$7 \times 7: u = 0, \sigma = 0.5$					

E. Parameters

LEA is compared with standard EA baselines (DE (DE/rand/1/bin) (Das & Suganthan, 2010), ES ((μ, λ) -ES), and CMA-ES), L2O-swarm (Cao et al., 2019) (a representative L2O method for black-box optimization), and Dragonfly (Kandasamy et al., 2020) (the state-of-the-art Bayesian optimization). DE and ES are implemented based on Geatpy (et.al., 2020), and CMA-ES

is implemented by Pymoo (Blank & Deb, 2020). The parameters of DE, ES, CMA-ES, and Dragonfly are adjusted to be optimal for each problem. L2O-swarm and LEA use the same training set and loss function. All algorithms are run ten times for each function. LEAws3 contains 3 EMs, and the parameters of these three convolution kernels are consistent across different EMs (weight sharing). The population sizes of DE, ES, CMA-ES, and LEA are 100. DE, ES, and CMA-ES run for 100 generations. For LEAws3, its architecture determines that LEA has only been iterated for three generations. DE, ES, and CMA-ES have 100/3 times as many function evaluations as LEA, which is highly unfair to LEA. Both Dragonfly and L2O-Swarm run to converge.

F. Visualization

We take a two-dimensional F4 function as an example to verify that LEA can indeed advance the optimization. In Figure 11, as the iteration proceeds, LEA gradually converges. When passing through the first EM module, the CRM is first passed, and the offspring S_{i-1} are widely distributed in the search space, and the offspring are closer to the optimal solution. Therefore, the CRM generates more potential offspring and is rich in diversity. After the SM update, the generated S_i is around the optimal solution, showing that the SM update can keep good solutions and remove poor ones. This phenomenon also leads to a vast improvement after passing through this module. From the population distribution results of the 2nd, 3rd, and 15th EMs, LEA continuously moves the population to the vicinity of the optimal solution.

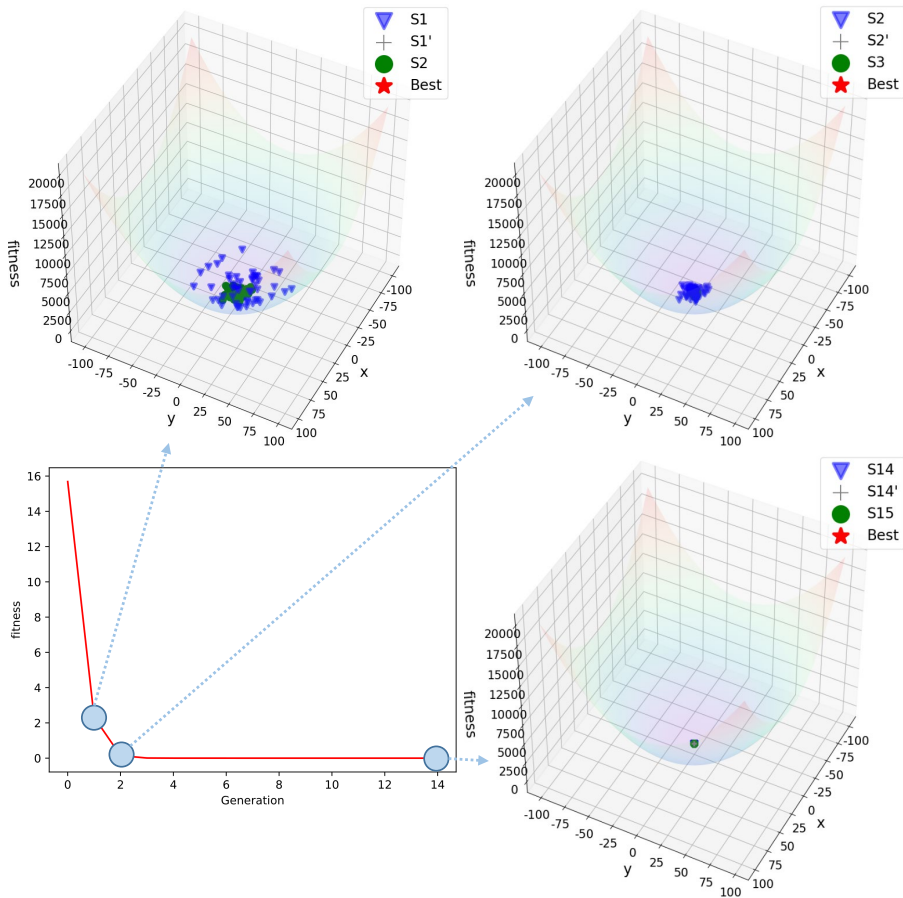


Figure 11. Visualization of the optimization process.

G. Comparison Results between LEAws30 and GAs

This section discusses the results to show the effectiveness of LEA compared with traditional GAs. The generation of these reference algorithms is set to 50, while LEAws30 only evolves the population with 30 EMs (30 generations).

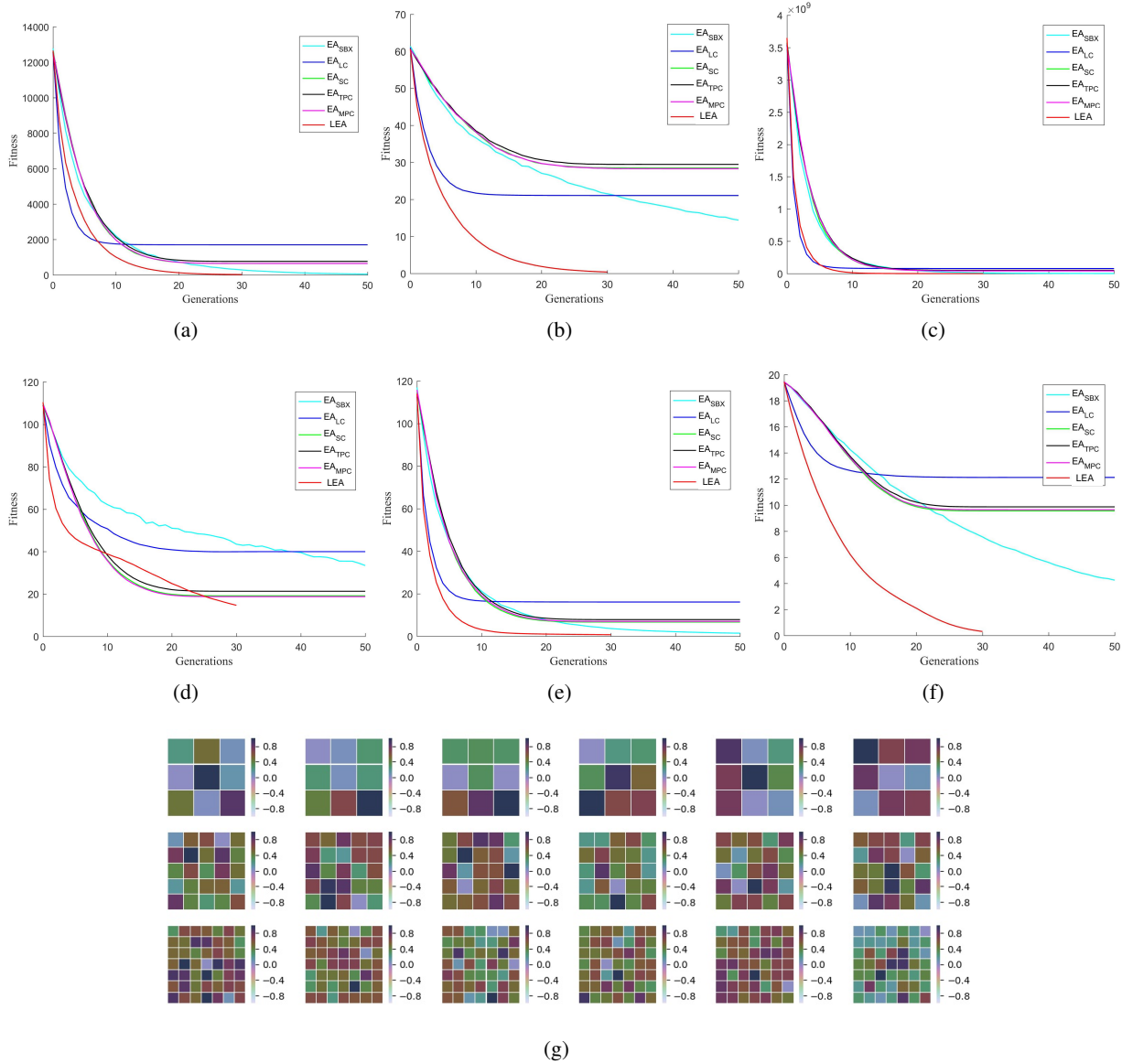


Figure 12. Experimental results are obtained upon different optimization tasks given in 8 when the dimension is 10. Results given in (a)-(f) are respectively obtained upon F4-F9. The generation of algorithms is set to 50, and LEA only evolves for 30 generations. This experimental results are obtained by averaging over 640 independent runs (batch size = 32). The corresponding heatmap of kernels in LEAs trained for these functions is also provided in (g).

The parameters within LEAws30 obtained subject to different objective functions are shown in the heatmap and are normalized within $[-1, 1]$ for each kernel. The results are provided in Table 12. As can be seen, for functions F4, F5, F6, F8, and F9, the converge curves of LEAws30 are below the curves of EASBX, EATPC, EAMPC, EASC, and EALC. For function F7, LEAws30 can avoid premature convergence. The performance of LEAws30 surpasses these human-designed recombination operators. In this case, the designed EM module can automatically learn optimization strategies similar to genetic operators without supervised information and obtain better performance than the human-designed recombination and selection operators.

Table 10. The detailed compared results between LEA and EALC on F4-F9 with different D and L .

D	F	L							
		10		20		40		80	
		EALC	LEAws3	EALC	LEA ws3	EALC	LEA ws3	EALC	LEA ws3
2	F4	1.05E+01	1.22E-01	1.80E+00	1.07E-02	4.56E-01	2.26E-03	1.12E-01	3.98E-04
	F5	2.50E+00	2.55E-01	1.02E+00	8.60E-02	5.15E-01	4.05E-02	2.64E-01	1.69E-02
	F6	2.63E+04	9.83E+00	8.66E+02	2.57E+00	5.23E+01	1.28E+00	8.67E+00	5.00E-01
	F7	2.27E+00	7.44E-01	9.72E-01	2.58E-01	3.79E-01	8.20E-02	9.93E-02	2.38E-02
	F8	6.10E-01	8.61E-02	2.73E-01	3.90E-02	1.36E-01	2.02E-02	7.02E-02	1.08E-02
	F9	3.83E+00	5.77E-01	2.44E+00	1.42E-01	1.33E+00	5.54E-02	5.02E-01	2.16E-02
10	F4	3.44E+03	8.49E+02	2.19E+03	2.77E+02	1.55E+03	9.54E+01	1.08E+03	4.24E+01
	F5	3.31E+01	1.70E+01	2.61E+01	1.11E+01	2.18E+01	6.67E+00	1.87E+01	4.61E+00
	F6	2.94E+08	2.75E+07	1.17E+08	2.93E+06	5.61E+07	4.15E+05	2.89E+07	6.06E+04
	F7	7.12E+01	5.18E+01	6.03E+01	4.43E+01	5.10E+01	3.78E+01	4.37E+01	3.32E+01
	F8	3.25E+01	7.97E+00	2.12E+01	3.21E+00	1.42E+01	2.02E+00	1.10E+01	1.36E+00
	F9	1.55E+01	1.14E+01	1.38E+01	7.26E+00	1.26E+01	5.33E+00	1.14E+01	4.24E+00
30	F4	2.30E+04	9.92E+03	1.83E+04	6.64E+03	1.60E+04	3.58E+03	1.38E+04	2.69E+03
	F5	5.77E+01	3.71E+01	5.15E+01	3.10E+01	4.76E+01	2.61E+01	4.43E+01	2.19E+01
	F6	4.43E+09	9.47E+08	2.85E+09	3.49E+08	2.03E+09	1.23E+08	1.60E+09	4.90E+07
	F7	3.03E+02	2.45E+02	2.77E+02	2.27E+02	2.58E+02	2.16E+02	2.43E+02	2.04E+02
	F8	2.04E+02	9.75E+01	1.66E+02	5.50E+01	1.44E+02	3.62E+01	1.26E+02	2.53E+01
	F9	1.83E+01	1.56E+01	1.77E+01	1.38E+01	1.72E+01	1.26E+01	1.67E+01	1.11E+01
50	F4	4.60E+04	2.42E+04	3.91E+04	1.65E+04	3.53E+04	1.13E+04	3.19E+04	8.23E+03
	F5	6.68E+01	4.43E+01	6.09E+01	3.80E+01	5.67E+01	3.47E+01	5.39E+01	3.14E+01
	F6	1.06E+10	2.57E+09	7.80E+09	1.15E+09	6.15E+09	6.24E+08	5.11E+09	2.89E+08
	F7	5.46E+02	4.54E+02	5.15E+02	4.26E+02	4.88E+02	4.09E+02	4.67E+02	3.97E+02
	F8	4.05E+02	2.22E+02	3.50E+02	1.40E+02	3.16E+02	1.10E+02	2.91E+02	8.04E+01
	F9	1.88E+01	1.68E+01	1.84E+01	1.57E+01	1.80E+01	1.47E+01	1.78E+01	1.36E+01
100	F4	1.07E+05	6.23E+04	9.55E+04	4.93E+04	8.93E+04	3.80E+04	8.39E+04	3.32E+04
	F5	7.65E+01	5.21E+01	7.15E+01	4.62E+01	6.81E+01	4.29E+01	6.50E+01	4.05E+01
	F6	2.86E+10	8.56E+09	2.28E+10	4.78E+09	1.97E+10	3.19E+09	1.73E+10	2.20E+09
	F7	1.18E+03	1.01E+03	1.13E+03	9.72E+02	1.09E+03	9.30E+02	1.06E+03	9.19E+02
	F8	9.70E+02	5.90E+02	8.61E+02	4.45E+02	8.03E+02	3.43E+02	7.53E+02	2.83E+02
	F9	1.93E+01	1.78E+01	1.90E+01	1.70E+01	1.88E+01	1.64E+01	1.86E+01	1.58E+01
500	F4	6.24E+05	4.13E+05	5.91E+05	3.62E+05	5.70E+05	3.28E+05	5.53E+05	2.98E+05
	F5	9.39E+01	6.28E+01	8.92E+01	5.72E+01	8.65E+01	5.57E+01	8.40E+01	5.45E+01
	F6	1.99E+11	6.78E+10	1.75E+11	5.18E+10	1.61E+11	4.27E+10	1.53E+11	3.76E+10
	F7	6.43E+03	5.69E+03	6.29E+03	5.57E+03	6.18E+03	5.48E+03	6.11E+03	5.43E+03
	F8	5.67E+03	3.67E+03	5.32E+03	3.23E+03	5.11E+03	2.96E+03	4.99E+03	2.73E+03
	F9	1.97E+01	1.85E+01	1.95E+01	1.82E+01	1.94E+01	1.80E+01	1.94E+01	1.78E+01

LEA is trained with the training set constructed with the same unimodal or multimodal function during the training process. The training process is relatively stable, and the test results are better for the same unimodal or multimodal function.

H. CEC2013

Similarly, F^{train} is produced based on functions in 7, and F^{test} is generated based on functions in CEC-2013 (Liang et al., 2013), where the dimension is set to 30. CEC-2013 is employed to validate that a trained LEA satisfies many other unseen objective functions (unseen during the training stage). Here, F^{test} is more complex than Table 8.

Unlike previous LEAs that share weights across different EMs, in this part, an LEA model without weight sharing (LEAnws) is trained because different individual interaction strategies may be required for offspring reproduction in each generation. The performance of EASBX, EATPC, EAMPC, EASC, and EALC is provided as references. We set the generation of these algorithms to 15. Also, 320 independent runs are conducted (batch size \times the number of repetitions: 16×20) to obtain the average performance of LEAnws15.

During the training process, LEA is trained with a training set constructed by mixing functions with different characteristics such as unimodal, multimodal, separable, and non-separable. The loss function fluctuates significantly during the training process, but the test results on the complex CEC2013 are still good. Thus, LEA has a good generalization ability. However, the advantage of LEA is not apparent for more complex optimization problems, such as CEC14, 15, and CEC22-27. These features are not available in the training set, such as the local optima's number being vast and the second better local optimum being far from the global optimum, continuous but differentiable only on a set of points and different properties around different local optima. LEA did not learn relevant processing experience, so it is easy to fall into the local optimum. Similarly, for CEC1-8, 10-13, 16-21, the training set does not have the following characteristics: quadratic ill-conditioned, smooth local irregularities, smooth but narrow ridge, with one sensitive direction, having a very narrow valley from local optimum to global optimum, local optima's number is huge, local optima's number is vast, non-continuous, rotated, asymmetrical, and continuous everywhere yet differentiable nowhere, but LEA has good generalization ability for problems with these characteristics. This case appears because these properties are less confusing about the location of the optimal solution. For the specific description and function characteristics of CEC2013, please refer to (Liang et al., 2013).

If the test set and the training set have a certain similarity in the representation, we can obtain a better generalization ability of LEA. If they are completely irrelevant, our scheme has no particular advantage.

Table 11. The Compared Results on CEC 2013.

Algorithm	CECF1	CECF2	CECF3	CECF4	CECF5	CECF6	CECF7
EATPC	1.99E+04	5.97E+08	1.42E+13	2.69E+05	1.17E+04	1.48E+03	7.48E+02
EAMPC	1.71E+04	6.38E+08	2.71E+12	3.70E+05	7.61E+03	1.06E+03	2.58E+02
EASC	1.73E+04	6.41E+08	3.24E+12	3.24E+05	7.59E+03	1.01E+03	3.86E+01
EALC	4.14E+04	8.59E+08	4.68E+18	7.35E+04	1.73E+04	7.98E+03	9.73E+05
EASBX	2.06E+04	6.69E+08	1.14E+15	3.89E+05	8.60E+03	1.79E+03	6.73E+03
LEAnws15	4.45E+03	1.43E+08	1.29E+11	6.45E+04	2.95E+03	1.53E+02	4.79E+02
Algorithm	CECF8	CECF9	CECF10	CECF11	CECF12	CECF13	CECF14
EATPC	6.79E+02	5.52E+02	3.21E+03	1.33E+02	2.48E+02	3.52E+02	5.13E+03
EAMPC	6.79E+02	5.52E+02	2.95E+03	8.15E+01	2.21E+02	3.19E+02	4.50E+03
EASC	6.79E+02	5.52E+02	2.99E+03	8.26E+01	2.20E+02	3.22E+02	4.50E+03
EALC	6.79E+02	5.56E+02	6.39E+03	2.87E+02	3.87E+02	4.83E+02	8.89E+03
EASBX	6.79E+02	5.52E+02	3.47E+03	1.58E+02	2.73E+02	3.71E+02	8.85E+03
LEAnws15	6.79E+02	5.54E+02	6.67E+02	6.13E+00	8.17E+01	1.85E+02	8.90E+03
Algorithm	CECF15	CECF16	CECF17	CECF18	CECF19	CECF20	CECF21
EATPC	9.53E+03	2.06E+02	1.25E+03	1.34E+03	2.25E+05	6.15E+02	3.72E+03
EAMPC	9.54E+03	2.06E+02	1.15E+03	1.26E+03	1.71E+05	6.15E+02	3.58E+03
EASC	9.55E+03	2.06E+02	1.15E+03	1.26E+03	1.80E+05	6.15E+02	3.61E+03
EALC	8.74E+03	2.06E+02	1.02E+03	1.13E+03	3.11E+05	6.15E+02	3.23E+03
EASBX	9.65E+03	2.06E+02	1.25E+03	1.35E+03	3.50E+05	6.15E+02	3.79E+03
LEAnws15	9.10E+03	2.05E+02	6.82E+02	7.91E+02	4.18E+03	6.15E+02	2.83E+03
Algorithm	CECF22	CECF23	CECF24	CECF25	CECF26	CECF27	CECF28
EATPC	7.22E+03	1.10E+04	1.33E+03	1.45E+03	1.61E+03	2.80E+03	6.57E+03
EAMPC	6.74E+03	1.10E+04	1.33E+03	1.44E+03	1.61E+03	2.80E+03	6.32E+03
EASC	6.86E+03	1.10E+04	1.33E+03	1.44E+03	1.62E+03	2.81E+03	6.33E+03
EALC	1.04E+04	1.06E+04	1.48E+03	1.45E+03	1.59E+03	2.93E+03	7.11E+03
EASBX	1.04E+04	1.11E+04	1.34E+03	1.46E+03	1.61E+03	2.82E+03	6.97E+03
LEAnws15	1.05E+04	1.06E+04	1.32E+03	1.44E+03	1.59E+03	2.75E+03	5.42E+03

I. Accelerate LEA with GPU

The acceleration of EAs using GPUs is challenging, and lots of research has contributed to this problem. The support for multiple subpopulations to evolve simultaneously has paramount significance in practical applications. The efforts (Jin & Qin, 2017; Qin et al., 2012) accelerated the K-Means process within the brain storm optimization algorithm through GPUs and proposed an improved CUDA-based implementation of differential evolution on GPUs. Many other EAs have benefited from the computing performance of GPUs (Huang et al., 2021; Cheng & Gen, 2019). However, all of them just parallelized

the current EAs. Besides, many available genetic operators are unfriendly to the GPU acceleration, as GPUs are weak in processing logical operations. As both CRM and SM are comprised of operations upon tensors, they can be sufficiently accelerated by GPUs.

LEA mainly containing operations upon tensors and is easily accelerated by GPUs. Current distributed EA methods usually separate a population into multiple subpopulations that evolve simultaneously. Such separation is also a commonly accepted operation in many EAs. However, none of them can accelerate the genetic operators. Here, we show the surprising performance of LEA with GPU accelerated CRM and SM. Moreover, Tensorflow has provided mature solutions for the acceleration upon GPUs, and LEA implemented by Tensorflow is supportable to load multiple populations as the input.

To show the adaptability of LEA to GPUs, we offer the runtime of LEA and unaccelerated EA in Table 12, within which both LEA and EA optimize $K = 32$ populations with each containing $L \times L$ individuals (number of individuals: $K \times L \times L$). Similarly, we employ the runtime of EASBX without acceleration as a reference in this experiment.

In the unified test environment, the function estimation time consumed by LEA and EA is basically the same. As can be seen, with the increase of L , the advantage of acceleration based on GPUs is clear. When the dimension $D \in \{2, 10\}$, LEA runs 103~104 times faster than EA. LEA is still around 102 times faster than EA when $D \in \{30, 50, 100, 500\}$. This case indicates that LEA is adapted to the acceleration of GPUs and can be accelerated sufficiently. However, with increasing D , LEA increases the proportion of evaluations in the runtime and ultimately weakens the advantage of acceleration. These cases indicate the acceleration advantage of LEA when optimizing a larger population. However, GPU cannot accelerate EA’s crossover, mutation, and selection modules. In the case of a large population of individuals, these operators take up a high running time.

Table 12. Investigation of LEA’s calculation efficiency when accelerated upon one 1080Ti GPU. The results in this table are the average time (second) of algorithms to conduct the evolution of 32 input populations for three generations.

D	ALGORITHM	L			
		10	20	40	80
2	LEA(s)	0.004627	0.005978	0.007449	0.015492
	EA(s)	0.700342	2.863495	12.67563	71.74005
	RATE(LEA/EA)	0.006607	0.002088	0.000588	0.000216
10	LEA	0.005487	0.007838	0.01664	0.049973
	EA	0.694213	2.879791	12.87636	72.3664
	RATE(EM/EA)	0.007904	0.002722	0.001292	0.000691
30	LEA	0.007052	0.013323	0.039877	0.138544
	EA	0.693307	2.87876	13.00381	71.67544
	RATE(EM/EA)	0.010171	0.004628	0.003067	0.001933
50	LEA	0.008026	0.01875	0.062079	0.237182
	EA	0.681967	2.868	12.80662	71.44253
	RATE(EM/EA)	0.011769	0.006538	0.004847	0.00332
100	LEA	0.011725	0.033109	0.117593	0.478518
	EA	0.699074	2.865546	13.12218	71.83043
	RATE(EM/EA)	0.016772	0.011554	0.008961	0.006662
500	LEA	0.041167	0.147843	0.610056	2.727426
	EA	0.720847	2.966926	13.59977	74.9417
	RATE(EM/EA)	0.057109	0.04983	0.044858	0.036394

J. Extensive Information for Protein Docking

Protein docking predicts the 3D structures of protein-protein complexes given individual proteins’ 3D structures or 1D sequences (Smith & Sternberg, 2002). We consider the *ab initio* protein docking problem (Smith & Sternberg, 2002), which is formulated as optimizing the Gibbs binding free energy for conformation s : $f(s) = \nabla G(s)$. We calculate the energy function in a CHARMM 19 force field as in (Moal & Bates, 2010). We parameterize the search space as $s \in R^{12}$ as in (Cao & Shen, 2020). We only consider 100 interface atoms. The training set includes 125 instances (see Appendix J), which contains 25 protein-protein complexes from the protein docking benchmark set 4.0 (Hwang et al., 2010), each of which has five starting points (top-5 models from ZDOCK (Pierce et al., 2014)). The testing set includes three complexes (with

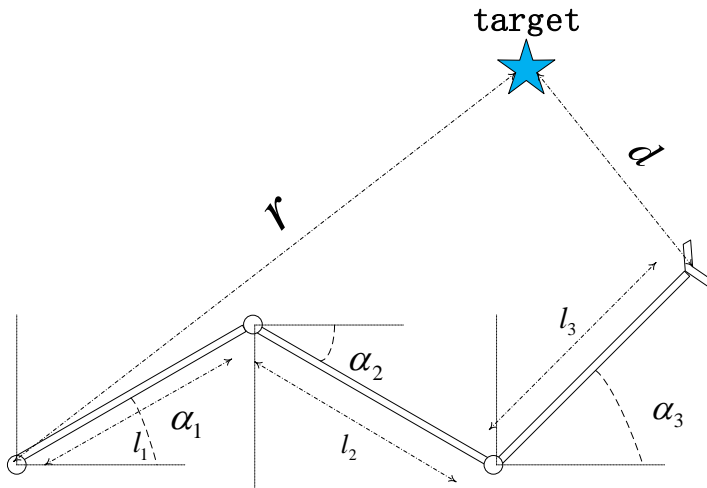


Figure 13. Planar Mechanical Arm.

one starting model each) of different levels of docking difficulty. 1ATN is the protein class that appeared during training. 1ATN_7 is the No. 7 instance of the 1ATN class, and it did not appear in the training process. 2JEL_1 and 7CEI_1 are the No. 1 instances of the two classes of proteins that did not participate in the training process.

The training dataset contains 25 protein-protein complexes from the protein docking benchmark set 4.0 (Hwang et al., 2010). The detailed information is shown as follows: 1ATN, 1AVX, 1AY7, 1BJ1, 1BVN, 1CGI, 1DFJ, 1EAW, 1EWY, 1EZU, 1GRN, 1IBR, 1IJK, 1IQD, 1JPS, 1KXQ, 1M10, 1MAH, 1N8O, 1PPE, 1R0R, 1XQS, 2B42, 2C0L, and 2HRK.

K. Extensive Information for Planner Mechanic Arm

The planner mechanic arm has been frequently employed as an optimization problem to assess how well the black-box optimization algorithms perform (Cully et al., 2015; Vassiliades et al., 2018; Vassiliades & Mouret, 2018; Mouret & Maguire, 2020). The planner mechanic arm problem has two key parameters: the set of $L = (L_1, L_2, \dots, L_n)$ and the set of angles $\alpha = (\alpha_1, \alpha_2, \dots, \alpha_n)$, where n represents the number of segments of the mechanic arm, and $L_i \in (0, 10)$ and $\alpha_i \in (-\Pi, \Pi)$ represent the length and angle of the i th mechanic arm, respectively. This problem is to find the suitable sets of L and α such that the distance $f(L, \alpha, p)$ from the top of the mechanic arm to the target position p is the smallest, where $f(L, \alpha, p) = \sqrt{(\sum_{i=1}^n \cos(\alpha_i)L_i - p_x)^2 + (\sum_{i=1}^n \sin(\alpha_i)L_i - p_y)^2}$, and (p_x, p_y) represents the target point's x- and y-coordinates. Here, $n = 100$. We design two groups of experiments.

L. Limitations

However, LEA has many drawbacks. We hope to address these deficiencies in future work.

- 1) The designed loss function enables LEA to perform the exploitation operation well but does not strongly encourage LEA to explore the fitness landscape. However, we have many options to balance exploration and exploitation. For example, the constructed Bayesian posterior distribution (Cao & Shen, 2020) over the global optimum is added to Eq. 5. In addition to adding items that focus on the exploration ability of the loss function, new modules can also be designed to be added to the EM to help LEA jump out of the local optimum.
- 2) LEA does not have an advantage for the constructed training dataset if it is utterly irrelevant to the optimization objective. Thus, establishing a suitable training dataset is essential.
- 3) LEA only focuses on continuous optimization problems without constraints. For problems such as expensive optimization, combinatorial optimization, constrained optimization, and multi-objective optimization, LEA needs to be adjusted according to the characteristics of the problem. LEA is a standard optimizer like vanilla DE, ES, GA, and PSO. In order to deal with different types of problems, we need to make different corrections to LEA. For example, to deal with expensive problems,

we need to build surrogate models to assist LEA. We need to redesign the CRM module to generate new feasible solutions for combinatorial optimization problems. For example, for TSP tasks, GNN may be a feasible option to generate new solutions instead of CRM. We can redesign the CRM module for constrained optimization problems to generate feasible solutions. Of course, the easiest way is to use constraint violations and fitness functions as criteria for selecting the next generation in the SM module.

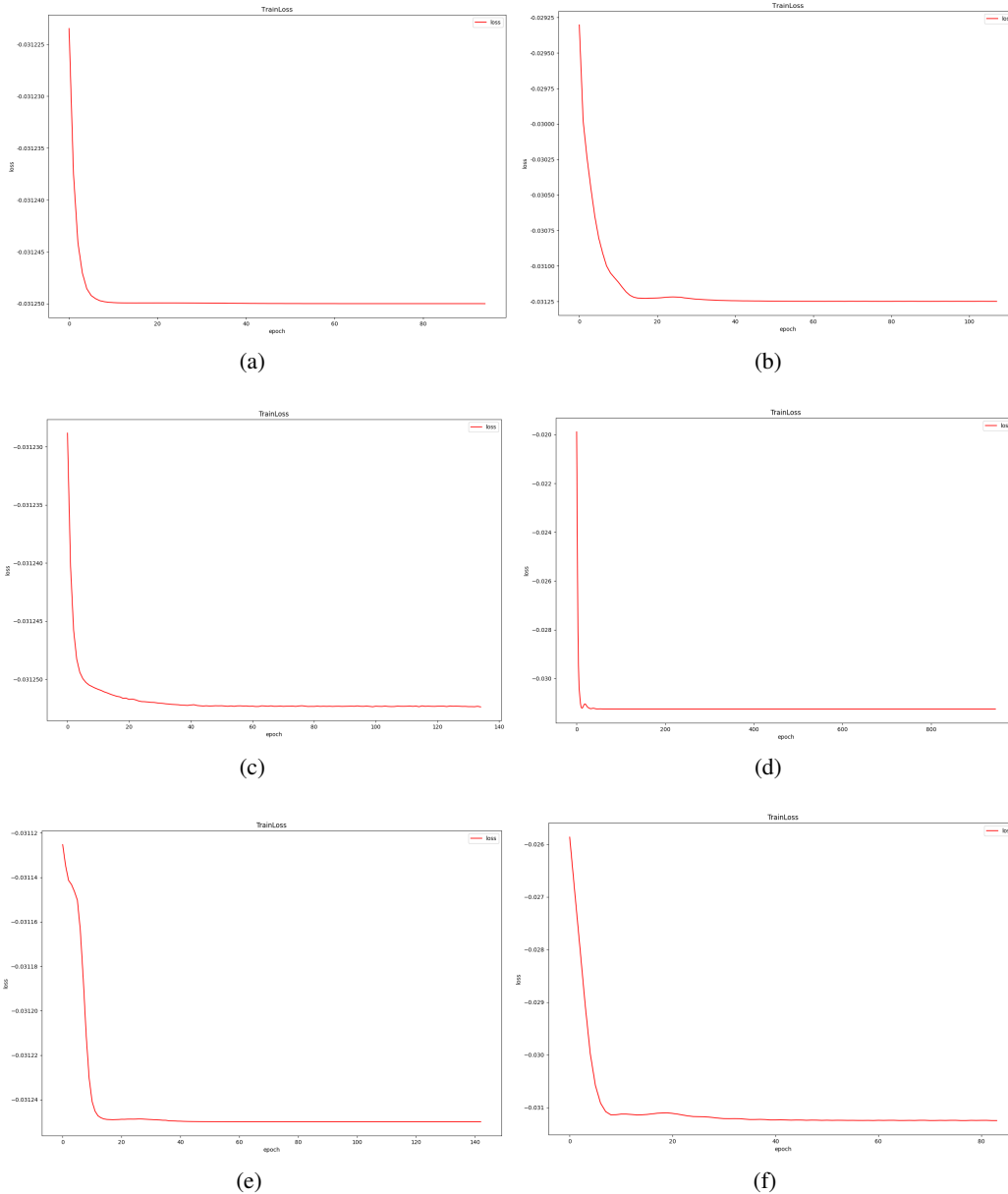


Figure 14. The convergence of loss function in training process. (a) F4, (b) F5, (c) F6, (d) F7, (e) F8, and (f) F9.

M. The Convergence of Loss Function in Training Process

This part is the change curve of the loss function of the training process of LEAnws15 on F4-F9. The results are shown in Figure 14. Here, $D=10$.